INTERFACE

rsif.royalsocietypublishing.org

Research

Cite this article: Cattalini JP, Hoppe A, Pishbin F, Roether J, Boccaccini AR, Lucangioli S, Mouriño V. 2015 Novel nanocomposite biomaterials with controlled copper/calcium release capability for bone tissue engineering multifunctional scaffolds. *J. R. Soc. Interface* **12**: 20150509.
http://dx.doi.org/10.1098/rsif.2015.0509

Received: 6 June 2015
Accepted: 20 July 2015

Subject Areas:
biomaterials, biomedical engineering, nanotechnology

Keywords:
alginate, angiogenesis, bioactive glass, bone tissue engineering, metal ion release, nanocomposites

Author for correspondence:
V. Mouriño
e-mail: vmourino@ffyb.uba.ar

Electronic supplementary material is available at http://dx.doi.org/10.1098/rsif.2015.0509 or via http://rsif.royalsocietypublishing.org.

THE ROYAL SOCIETY PUBLISHING

Novel nanocomposite biomaterials with controlled copper/calcium release capability for bone tissue engineering multifunctional scaffolds

J. P. Cattalini[1], A. Hoppe[2], F. Pishbin[4], J. Roether[3], A. R. Boccaccini[2], S. Lucangioli[1,5] and V. Mouriño[1,5]

[1]Department of Pharmaceutical Technology, Faculty of Pharmacy and Biochemistry, University of Buenos Aires, 956 Junín 6th floor, PC1113, Buenos Aires, Argentina
[2]Institute of Biomaterials, and [3]Institute of Polymer Materials, Department of Materials Science and Engineering, University of Erlangen-Nuremberg, Erlangen 91058, Germany
[4]Department of Materials, Imperial College London, Prince Consort Road, London SW7 2AZ, UK
[5]National Research Council (CONICET), Buenos Aires, Argentina

This work aimed to develop novel composite biomaterials for bone tissue engineering (BTE) made of bioactive glass nanoparticles (Nbg) and alginate cross-linked with Cu^{2+} or Ca^{2+} (AlgNbgCu, AlgNbgCa, respectively). Two-dimensional scaffolds were prepared and the nanocomposite biomaterials were characterized in terms of morphology, mechanical strength, bioactivity, biodegradability, swelling capacity, release profile of the cross-linking cations and angiogenic properties. It was found that both Cu^{2+} and Ca^{2+} are released in a controlled and sustained manner with no burst release observed. Finally, *in vitro* results indicated that the bioactive ions released from both nanocomposite biomaterials were able to stimulate the differentiation of rat bone marrow-derived mesenchymal stem cells towards the osteogenic lineage. In addition, the typical endothelial cell property of forming tubes in Matrigel was observed for human umbilical vein endothelial cells when in contact with the novel biomaterials, particularly AlgNbgCu, which indicates their angiogenic properties. Hence, novel nanocomposite biomaterials made of Nbg and alginate cross-linked with Cu^{2+} or Ca^{2+} were developed with potential applications for preparation of multifunctional scaffolds for BTE.

1. Introduction

Biomaterials that resemble the calcified bone matrix are frequently used to develop scaffolds for bone tissue engineering (BTE) [1–4]. Both inorganic and organic biomaterials (such as ceramics and polymers, respectively) have been widely used to prepare scaffolds with those requirements [3,5–9].

Among ceramics, bioactive glasses—particularly Bioglass® 45S5—exhibit interesting properties for BTE [7,8,10–14], such as the promotion of the formation of bone-like hydroxyapatite (HA) layers on the biomaterial surface [15,16], and their osteoconductive and osteoinductive characteristics [6,17,18]. In addition, reports indicate that dissolution products from bioactive glasses upregulate the expression of genes that control osteogenesis [13,17–19] and induce pro-angiogenic effects by stimulating the production of vascular endothelial growth factor (VEGF) [20,21], the secretion of angiogenic growth factors in fibroblasts [22,23], the proliferation of endothelial cells [22–24] and the formation of endothelial tubules [22]. Further, the reduction in size to the nanometre scale of bioactive glasses of nominal composition similar to Bioglass® 45S5 offers many advantages *in vitro*, such as higher protein adsorption capability and enhanced bioactivity, as well as faster HA deposition or mineralization of tissues in comparison with microparticles of the same composition [25–28].

Organic polymers have also been widely used to prepare porous scaffolds for BTE [11,29–31]. Particularly, natural polymers exhibit high biocompatibility and low tissue damage [30,32]. Among available natural, biocompatible polymers, alginates are widely used in tissue engineering [33–39] and drug delivery [37,39–41], because of their ability to form hydrogels when multivalent cations react with their guluronic residues [40,42]. As cross-linked alginate gels degrade, cross-linking ions are released due to the exchange with monovalent cations from the media [42]. Based on this fact, our group envisaged the possibility to control the release of the chosen multivalent ions in a sustained manner from a cross-linked site. In that sense, gallium cross-linked alginate/nanoparticulate bioactive glass composite two-dimensional (2D) scaffolds were successfully developed [43]. In addition, the incorporation of metallic ions into scaffolds for tissue engineering is being increasingly considered [35,43–49]. In particular, studies confirmed that calcium (Ca^{2+}) ions promote the differentiation of bone cells, the proliferation of osteoblasts, and the mineralization and metabolism of bone tissue [50,51]. Moreover, copper (Cu^{2+}) ions are considered metallic angiogenic factors, because of their important role in blood vessel growth [21,52–54] and the stimulation of the proliferation of endothelial cells [21,55–58]. In addition, Cu^{2+} ions also enhance the differentiation of stem cells towards the osteogenic linage [54,59]. Furthermore, Cu^{2+} is a natural antimicrobial material [45,47] and also reported was a synergistic antimicrobial effect with Ca^{2+} [60].

The possibility to combine both bioactive glass nanoparticles (Nbg) and alginate (Alg) allows synergizing the advantages of these biomaterials to develop composite scaffolds for BTE with suitable properties such as biodegradability, biocompatibility and mechanical strength [43,61,62]. This work builds upon the mentioned previous work of gallium cross-linked alginate/nanoparticulate bioactive glass composite 2D scaffolds, focusing on novel combinations of Nbg and Alg to achieve tuneable release capabilities of divalent ions—such as Cu^{2+} and Ca^{2+}—incorporated by cross-linking them with Alg in the composite biomaterials. The way in which the cross-linked ions were released and the effects of the dissolution products on blood vessels and bone formation were investigated. Novel nanocomposite biomaterials made of Nbg and Alg cross-linked with Cu^{2+} or Ca^{2+} with special focus on controlling the release of cross-linked ions in a sustained manner were developed with potential applications in the preparation of multifunctional scaffolds for BTE.

2. Materials

Nbg with nominal composition close to Bioglass® 45S5 (46 wt% SiO_2, 27 wt% CaO, 23 wt% Na_2O, 4 wt% P_2O_5), with spherical shape and mean particle size 35–40 nm, were a gift of D. Mohn and Prof. W. Stark (Swiss Federal Institute of Technology Zurich, Switzerland). Nbg were prepared by flame spray method [63] and have been characterized recently [27]. Sodium alginate (Protanal LF 10/60) was from FMC Biopolymers. HCl was from Sigma Aldrich. NaH_2PO_4 and $NH_4H_2PO_4$ were also from Sigma Aldrich and were used to prepare phosphate buffer solutions. $CuSO_4.5H_2O$ was from Fluka and $CaCl_2.2H_2O$ was from Merck. Silicone moulds were used to prepare 2D scaffolds. The water used was purified by distillation and deionization (MilliQ). A Denver Instrument UB10 pH meter was used.

3. Methods

3.1. Preparation of two-dimensional scaffolds

An Alg solution was prepared by dissolving Alg in a ratio of deionized water under magnetic stirring. An aqueous dispersion of Nbg was prepared by adding Nbg in deionized water, which was acidified with 1 M HCl and sonicated. This aqueous dispersion was added to the Alg solution previously prepared to obtain an AlgNbg mix, which was stirred continuously. The mix was adjusted to pH 7.4 with 1 M HCl and then was completed to final volume with deionized water to achieve a concentration of 2% w/v for Alg and 0.5% w/v for Nbg. The AlgNbg mix prepared was cast into moulds and left to dry for 24 h in order to obtain AlgNbg 2D scaffolds. Also, an Alg solution at 2% w/v was cast into moulds and left to dry for 24 h to obtain Alg 2D scaffolds. Then, both types of 2D scaffolds were cross-linked by immersing them into 2% w/v solutions of Cu^{2+} or Ca^{2+} ions for 1 h. Two-dimensional scaffolds were washed with deionized water and the excess water was removed by using a filter paper. Then, 2D scaffolds were dried in an oven at 25°C until 30% of weight loss. Finally, 2D scaffolds were kept in a sealed container at 25°C under 40% humidity. Four types of 2D scaffolds were obtained: AlgNbgCu, AlgNbgCa, AlgCu and AlgCa (figure 1).

3.2. Characterization

Morphology features were observed by scanning electron microscopy (SEM) (Zeiss Leica, Germany). Samples were gold-coated and observed at an accelerating potential of 5 kV. Potassium bromide (KBr) tablets were prepared for Fourier transform infrared (FTIR) spectroscopy from Alg and Nbg powders, and from AlgNbgCu and AlgNbgCa (previously pulverized to a fine powder). Briefly, the powders were mixed with KBr, pressed at 200 MPa to obtain tablets and analysed by a FTIR Nicolet 380 spectrometer. Mechanical properties of the 2D scaffolds were evaluated by measuring the tensile strength with a computer-controlled universal testing machine (Instron 1022) at a speed of 1 mm min^{-1}.

3.3. Acelluar *in vitro* study

In vitro bioactivity study of 2D scaffolds was carried out by immersing AlgNbgCu and AlgNbgCa in simulated body fluid (SBF) [16] at 37°C for 7 days. At certain intervals, 2D scaffolds were removed from the SBF, washed with deionized water and dried at 37°C for 30 min. The growth of HA crystals on 2D scaffold surfaces was determined by SEM and confirmed by X-ray diffraction (XRD). AlgCu and AlgCa were also immersed in SBF, as a negative control.

3.4. Degradation study

The degradation of 2D scaffolds was studied by analysing the weight loss of AlgNbgCu, AlgNbgCa, AlgCu and AlgCa. At first, 2D scaffolds were dried until constant weight was reached in an oven at 37°C (W_i, initial weight of 2D scaffolds before immersing in buffer) and immersed in phosphate buffer (10 ml, pH 7.4) at 37°C for 60 days. Two-dimensional scaffolds were taken at several intervals; the excess buffer was removed by using a filter paper and dried until constant weight (W_d, dried weight of 2D scaffolds after immersing in buffer) in an oven at 37°C. Five samples of each film type were used for each time interval studied. The percentage weight loss (%W_l) was obtained as follows:

$$\%W_l = \frac{W_i - W_d}{W_i} \times 100.$$

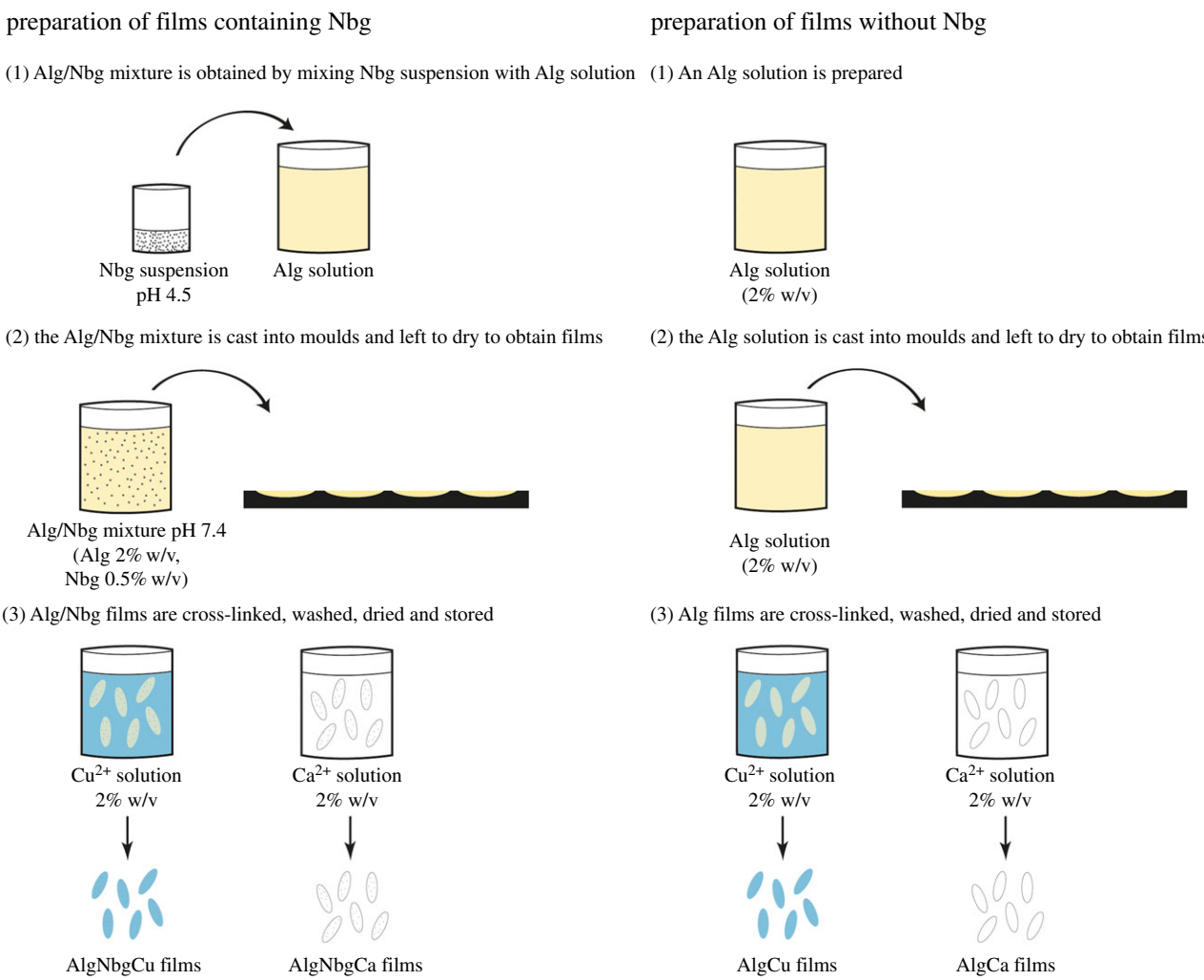

Figure 1. The preparation of the different types of 2D scaffolds. (Online version in colour.)

3.5. Swelling study

The swelling capacity was studied by analysing the weight gain of AlgNbgCu, AlgNbgCa, AlgCu and AlgCa. At first, 2D scaffolds were weighed (W_i, initial weight of 2D scaffolds before immersing in buffer) and immersed in phosphate buffer (10 ml, pH 7.4) at 37°C for 15 days. Two-dimensional scaffolds were taken at several intervals, the excess buffer was removed by using a filter paper, weighed (W_f, final weight of 2D scaffolds after removing the excess buffer) and re-immersed. Five samples of each film type were used. The percentage weight gain ($\%W_g$) was obtained as follows:

$$\%W_g = \frac{W_f - W_i}{W_i} \times 100.$$

3.6. pH control

AlgNbgCu, AlgNbgCa, AlgCu and AlgCa were immersed in phosphate buffer (10 ml, pH 7.4) at 37°C for 3 days in order to evaluate whether the Nbg incorporated would affect the pH value of the buffer solution. At several time intervals, 2D scaffolds were removed and the pH of the buffer solution was measured. Then, 2D scaffolds were re-immersed in phosphate buffer. pH determinations were performed for five samples of each type of film.

3.7. Release study of Cu^{2+} and Ca^{2+} ions

Cu^{2+} ion release from AlgNbgCu and AlgCu was studied in phosphate buffer (10 mM, pH 7.4) at 37°C for 60 days and quantified by a capillary electrophoresis method adapted from Baraj *et al.* [64]. Similarly, Ca^{2+} ion release from AlgNbgCa and AlgCa was studied in phosphate buffer (10 mM, pH 7.4) at 37°C for 60 days and quantified by a new capillary electrophoresis method recently reported [65]. Five samples of each film type were tested. Aliquots were withdrawn from the release study at regular intervals (2, 4, 8, 24, 48 h and then 7, 10, 14, 21, 35, 43, 50, 57 and 64 days) and 2D scaffolds were re-immersed in fresh buffer. Calibration curves were made in the range of 0.2–10 μg ml^{-1}.

3.8. *In vitro* cellular study

3.8.1. Preparation of biomaterial extracts

Extracts of AlgNbgCu and AlgNbgCa were prepared according to the International Organization for Standardization (ISO 10993-12). Briefly, the 2D scaffolds were incubated for 1, 10, 21, 43 and 64 days at 37°C in low-glucose Dulbecco's modified Eagle medium (L-DMEM) (Hyclone, USA) or endothelial cell medium (ECM) (Sciencell, San Diego, CA, USA). The ratio of the 2D scaffolds to the medium was 100 mg ml^{-1}. Cultures of cells in the presence of a range of ionic concentrations of calcium or copper introduced directly in the culture media were used as controls (ControlCa and ControlCu, respectively). The ion concentrations of calcium or copper used were those obtained from the release studies according to §3.7 for each period of incubation. Extracts of AlgCu and AlgCa were also prepared as control samples. Five samples of each type of film were used and the extracts were renewed at each medium change during cell culture.

3.8.2. Cell preparation and culture

Rat bone marrow-derived mesenchymal stem cells (rBMSCs) were obtained from the femora of four-week-old Sprague Dawley rats, as previously described [66]. Briefly, marrow of the femora midshaft was flushed out and suspended in L-DMEM supplemented with 10% fetal bovine serum (Hyclone), 100 U ml^{-1} penicillin and 100 mg l^{-1} streptomycin (Hyclone). Non-adherent cells were removed after 3 days. When reached approximately 80% confluence, cells were passaged and used for the following experiments from second to third passages.

Human umbilical vein endothelial cells (HUVECs) were isolated and cultured as described previously, with written informed consent of the donors [21]. Briefly, the umbilical vein was digested with 0.1% collagenase I (Sigma, St Louis, MO, USA) for 15 min at 37°C. Subsequently, the cells were collected and cultured in ECM (Sciencell). Non-adherent cells were removed after 24 h. HUVECs between the third and sixth passage were used in experiments.

3.8.3. Cell viability assays

Cell viability was evaluated by 3-(4,5-dimethylthiazol-2-yl)-2,5-diphenyltetrazolium bromide (MTT) colorimetric assay. Briefly, cells were seeded in 96-well plates at 3.1×10^4 cells cm^{-2}. The extracts described above, §3.8.1, were added, respectively, and incubated for 24 h. The MTT assay (Sigma) was performed following manufacturer's instructions. Dimethyl sulfoxide (Sigma) was used to dissolve the formazan crystals, and optical density was measured at 570 and 630 nm using a microplate reader (Labsystems Dragon Wellscan MK3, Finland).

3.8.4. Alkaline phosphatase staining and activity assay

Alkaline phosphatase (ALP) staining was performed using a BCIP/NBT ALP kit (Beyotime, Shanghai, China). Briefly, the rBMSCs were plated in 6-well plates and cultured for 10 days with different extracts as per indicated in §3.8.1. After fixation with 4% paraformaldehyde, the cells were incubated in a mixture of nitro-blue tetrazolium and 5-bromo-4-chloro-3-indolylphosphate [67]. ALP activity was assessed using ALP Detection Kit (Jiancheng Technology, Nanjing, China). Control samples were also assayed. The ALP activity was examined according to the manufacturer's instructions and normalized to the total protein content determined using BCA method as previously described [68].

3.8.5. Matrigel two-dimensional assay

For analysis of capillary tube formation, 75 ml of Matrigel (Becton Dickinson, UK) was pipetted into a 96-well plate (Falcon, Heidelberg, Germany) and incubated at 37°C for 60 min. HDMECs were harvested at week 1 or week 2 of being in contact with the material extract (different ranges of material extracts were used as per §3.8.1) and suspended at 50 000 cells per 150 ml of ECM. One hundred and fifty millilitres of this media were added to the Matrigel-coated 96-well plates and incubated for 24 h at 37°C. Capillary tube formation on Matrigel was observed at the end under an inverted Leica DMIL microscope and photos were taken using the Leica application suite software (Leica GmbH, Wetzlar, Germany).

3.9. Statistical analysis

Reported data from studies are presented as the mean ± s.e.m. (standard error of the mean) or the mean ± s.d. (standard deviation). ANOVA was performed when different results were compared.

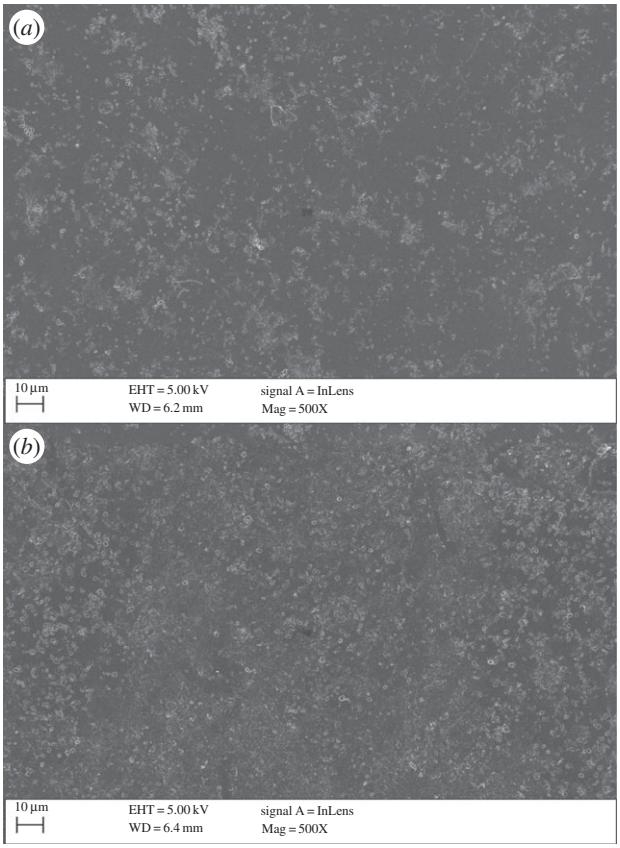

Figure 2. SEM images of the surface of 2D scaffolds before bioactivity studies: (*a*) AlgNbgCu 2D scaffolds and (*b*) AlgNbgCa 2D scaffolds.

4. Results

4.1. Characterization

SEM pictures show that matrices from both AlgNbgCu and AlgNbgCa 2D scaffolds were uniform and homogeneous (figure 2*a*,*b*, respectively). FTIR spectra are shown figure 3. Alg exhibited characteristic absorption bands at 3450 cm^{-1} from hydroxyl groups (OH), 1615 and 1410 cm^{-1} from asymmetric and symmetric stretching vibrations of carboxyl groups (COO), respectively, and 1125, 1080 and 1030 cm^{-1} due to stretching vibrations of C–C and C–O groups. FTIR spectrum for Nbg showed bands at around 1030 and 500 cm^{-1} from asymmetric and symmetric vibrations of Si–O–Si of the SiO_4 tetrahedra, respectively [69], the peak at around 900 cm^{-1} can be assigned to the SiO_{NBO} (non-bonding oxygen, NBO) [27] and the band that can be observed at 1450 cm^{-1} would be attributed to the carbonates that are adsorbed on the surface [27,70]. FTIR spectra of cross-linked composite 2D scaffolds showed intense bands from both the Alg and Nbg, and a slight shift in almost all the absorption bands was observed when compared with the Alg spectrum, where narrower intensity bands for OH and COO groups are seen in the spectra of AlgNbgCu and AlgNbgCa. It is also important to notice that almost all the absorption bands for AlgNbgCa are broader than those of AlgNbgCu. The analysis of the peaks from vibrations of C–C and C–O groups is rendered difficult not only due to the overlapping of the peak at 1125 cm^{-1} with the peak at 1080 cm^{-1}, but also due to the overlapping of these bands with the asymmetric vibrations of Si–O–Si groups from Nbg. The effect of Nbg incorporation into the 2D scaffolds on tensile strength is shown in figure 4

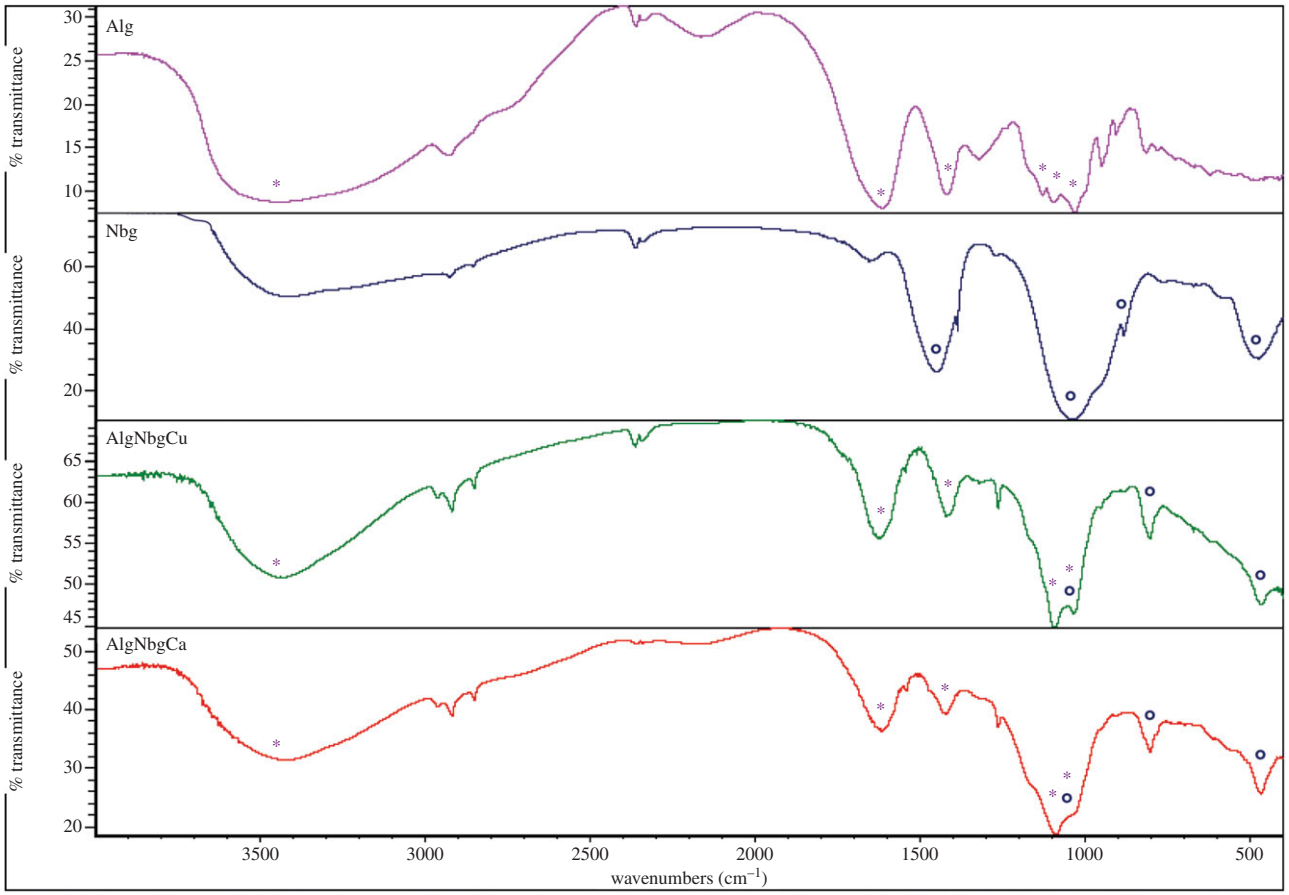

Figure 3. FTIR spectra of Alg, Nbg, AlgNbgCu 2D scaffolds and AlgNbgCa 2D scaffolds. The absorption bands for Alg and Nbg are indicated as symbols (*) and (°), respectively. (Online version in colour.)

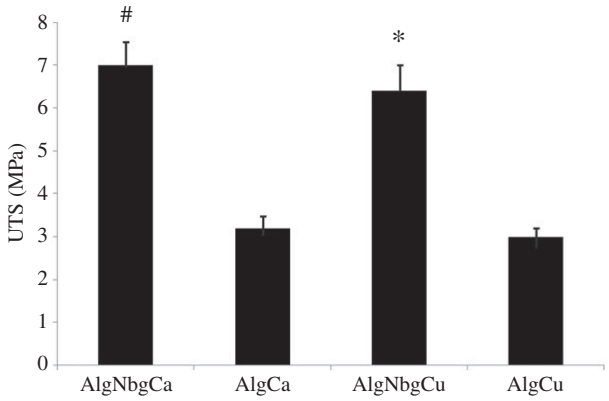

Figure 4. Values of UTS of AlgNbgCu, AlgNbgCa, AlgCu and AlgCa 2D scaffolds. The incorporation of Nbg into the 2D scaffolds resulted in a significant increase in the UTS. Significantly different from *AlgCu 2D scaffolds and #AlgCa 2D scaffolds ($p < 0.05$). Average values $\pm$ s.d.

where the point of failure or ultimate strength (UTS) of different samples is charted. AlgNbgCu and AlgNbgCa showed a significant increase ($p < 0.05$) in the UTS in comparison with those 2D scaffolds without Nbg.

4.2. Acellular *in vitro* study

After 3 days of immersion in SBF, the growth of crystals was observed on the surface of both AlgNbgCu and AlgNbgCa (data not shown). After 7 days of immersion in SBF, SEM images indicated that the amount of crystals on the surface increased (figure 5*a*,*b*) and the XRD spectrum showed sharp peaks at 31.8° and 46.7° attributed to 211 and 222 plane of HA [71] (figure 5*b*). AlgCu and AlgCa did not show any deposition of HA crystals on their surfaces (figure 5*c*) and no peaks corresponding to any crystallization were observed by XRD studies.

4.3. Degradation, swelling and pH control

The degradation profile of all samples is shown in figure 6*a*. AlgNbgCa and AlgCa did not show any significant variation in their weight loss and they still remained shaped until the end of the study, whereas AlgNbgCu and AlgCu degraded at a higher rate which was more notable after day 40. A weight loss of 42.7% was observed for AlgNbgCu at the end of the study. Swelling study showed a weight gain of about 100% for both AlgNbgCa and AlgCa (figure 6*b*). On the other hand, AlgNbgCu and AlgCu showed no significant changes in their weight during the swelling study (figure 6*b*). No significant changes were observed in the pH value of the buffer solution where AlgNbgCu and AlgCu were immersed (figure 6*c*). Otherwise, there was a slight increase in the pH value of the buffer solution (initially 7.4) where AlgNbgCa and AlgCa 2D were immersed, where the highest pH values were 7.57 and 7.54, respectively (figure 6*c*).

4.4. Release study of Cu^{2+} and Ca^{2+} ions

The study of the release profile of Ca^{2+} ions (figure 7) showed no significant differences for both AlgNbgCa and AlgCa. The amount of Ca^{2+} ions released in each time point increased steadily during the first three weeks of the study. After that

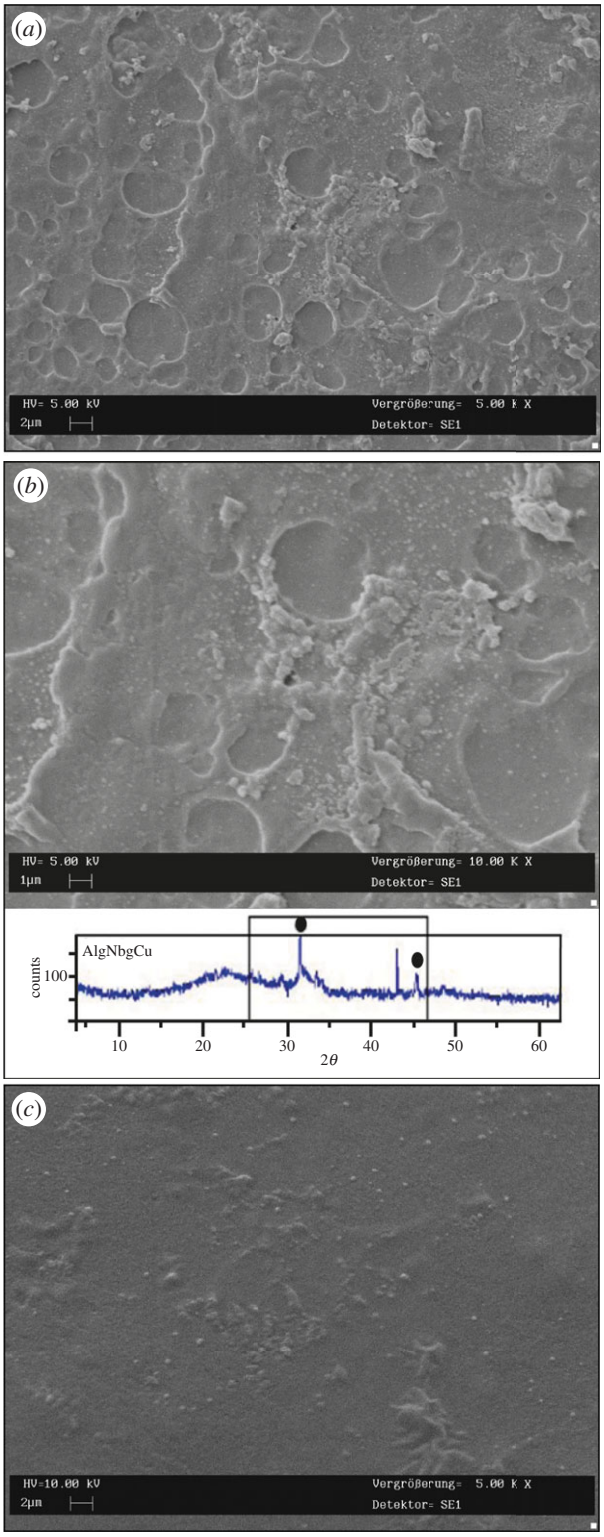

Figure 5. SEM pictures showing crystals formed on the surface of 2D scaffolds after 7 days of immersion in SBF: (*a*) low magnification (sample: AlgNbgCu); (*b*) high magnification. The bottom part of the image shows the XRD spectrum where sharp peaks at 31.8° and 46.7° could be attributed to HA crystals on the surface of the nanocomposite 2D scaffolds after 7 days in SBF (sample: AlgNbgCu). Similar results were obtained for AlgNbgCa. (*c*) Any crystals were observed on the surface of 2D scaffolds without Nbg (sample: AlgCu). (Online version in colour.)

and until the end of the study, a slight decrease in the amount of Ca^{2+} ions released can be noted. After two months, the total amount of Ca^{2+} ions released from both 2D scaffolds was in the range 30–32 µg ml^{-1}. The release profile of Cu^{2+} ions (figure 7) showed that the amount released in each time point was lower than the amount of Ca^{2+} ions released from AlgNbgCa and AlgCa. No differences between the amounts of Cu^{2+} ions released were found for both AlgNbgCu and AlgCu until day 21, where Cu^{2+} ions were slowly released without any burst effect. From day 37 to 57, AlgNbgCu released a higher amount of Cu^{2+} ions than AlgCu. After two months, the total amount of Cu^{2+} ions released from both 2D scaffolds was 22–24 µg ml^{-1}.

4.5. *In vitro* cellular studies

4.5.1. Proliferation of rat bone marrow-derived mesenchymal stem cells cultured with AlgNbgCu and AlgNbgCa two-dimensional scaffold extracts

rBMSCs treated with extracts of AlgNbgCu and AlgNbgCa were the most metabolically active ($p < 0.005$) when compared with the ion concentration of calcium or copper, respectively, obtained from the release studies (see above, §4.4) for each period of incubation and when compared with AlgCu and AlgCa, respectively. In addition, the extracts of AlgCu and AlgCa did not significantly affect cell metabolic activity and growth compared with L-DMEM. No significant differences in cell metabolic activity were observed for cells cultured in the extracts of AlgNbgCu and AlgNbgCa for the periods studied. Figure 8*a* shows the results for rBMSCs treated with extracts of AlgNbgCu and AlgNbgCa obtained after 24 h of soaking.

4.5.2. Osteogenic differentiation of rat bone marrow-derived mesenchymal stem cells cultured with AlgNbgCu and AlgNbgCa extracts

To investigate whether AlgNbgCu and AlgNbgCa extracts could affect the osteogenic differentiation of rBMSCs, ALP activity was examined. Interestingly, a time-dependent increase in ALP activity was observed for cells cultured in the extracts of AlgNbgCu and AlgNbgCa in the absence of osteogenic factors. ALP activity was not significantly different when the effects of AlgNbgCa and AlgNbgCu were compared with the ones of the ion concentrations of calcium or copper, respectively, obtained from the release studies (see above, §4.4) for each period of incubation and when compared with the ones of AlgCu and AlgCa, respectively, at day 3. However, ALP activity was significantly higher ($p < 0.001$) in cells cultured with the extracts of AlgNbgCu and AlgNbgCa after 10 days (figure 8*b*).

No significant differences in ALP activity were observed for cells cultured in the extracts of AlgNbgCu and AlgNbgCa.

4.5.3. Effect of AlgNbgCu and AlgNbgCa extracts on human umbilical vein endothelial cell function

To understand the interactions of AlgNbgCu and AlgNbgCa extracts with HUVECs, cell proliferation and the capability of forming tubes in Matrigel were analysed. Significant increase of cell viability ($p < 0.005$) was observed when incubated with AlgNbgCu and AlgNbgCa extracts obtained at different timepoints of material incubation—as detailed in §3.8.1—compared to AlgCu and AlgCa extracts, respectively; to ControlCu and ControlCa, respectively; and control. Figure 9*a* shows the results obtained when HUVECs were in contact with AlgNbgCu and AlgNbgCa extracts collected after 24 h of incubation compared to AlgCu and AlgCa, respectively, and

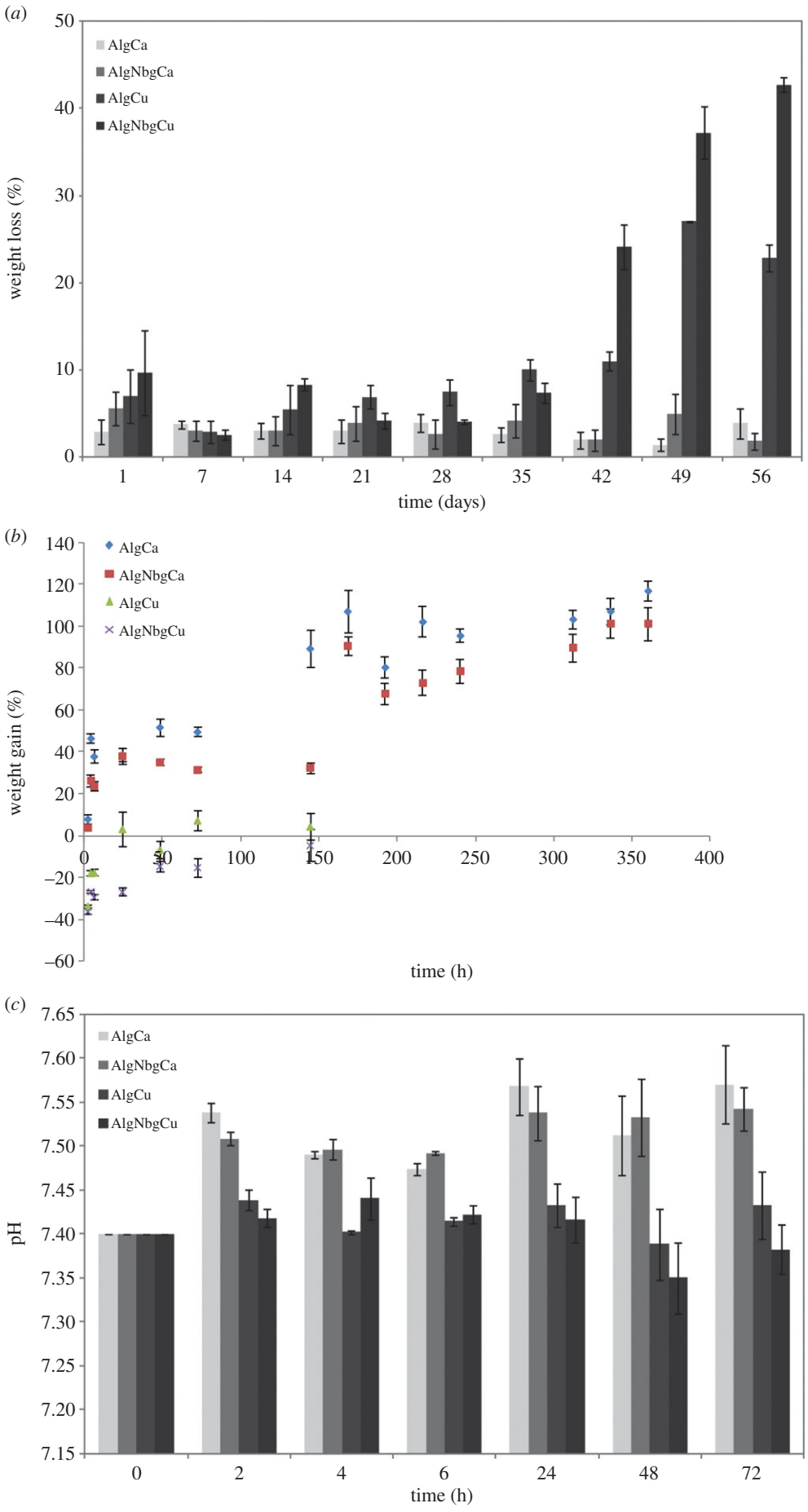

Figure 6. (*a*) Degradation study of AlgNbgCa and AlgCa 2D scaffolds showed no significant weight loss until the end of the study. Degradation study of AlgNbgCu and AlgCu 2D scaffolds showed that 2D scaffolds degraded at a higher rate than AlgNbgCa and AlgCa 2D scaffolds, which was more notable after day 40. (*b*) Swelling study of AlgNbgCa and AlgCa 2D scaffolds showed a weight gain of about 100%. Swelling study of AlgNbgCu and AlgCu 2D scaffolds showed no significant changes in their weight. (*c*) Whereas the pH values of the buffer solution where AlgCa and AlgNbgCa 2D scaffolds were immersed showed a slight increase, the pH values of the buffer solution where AlgNbgCu and AlgCu 2D scaffolds were immersed did not vary significantly. Average values $\pm$ s.e.m. are shown in all the graphics. (Online version in colour.)

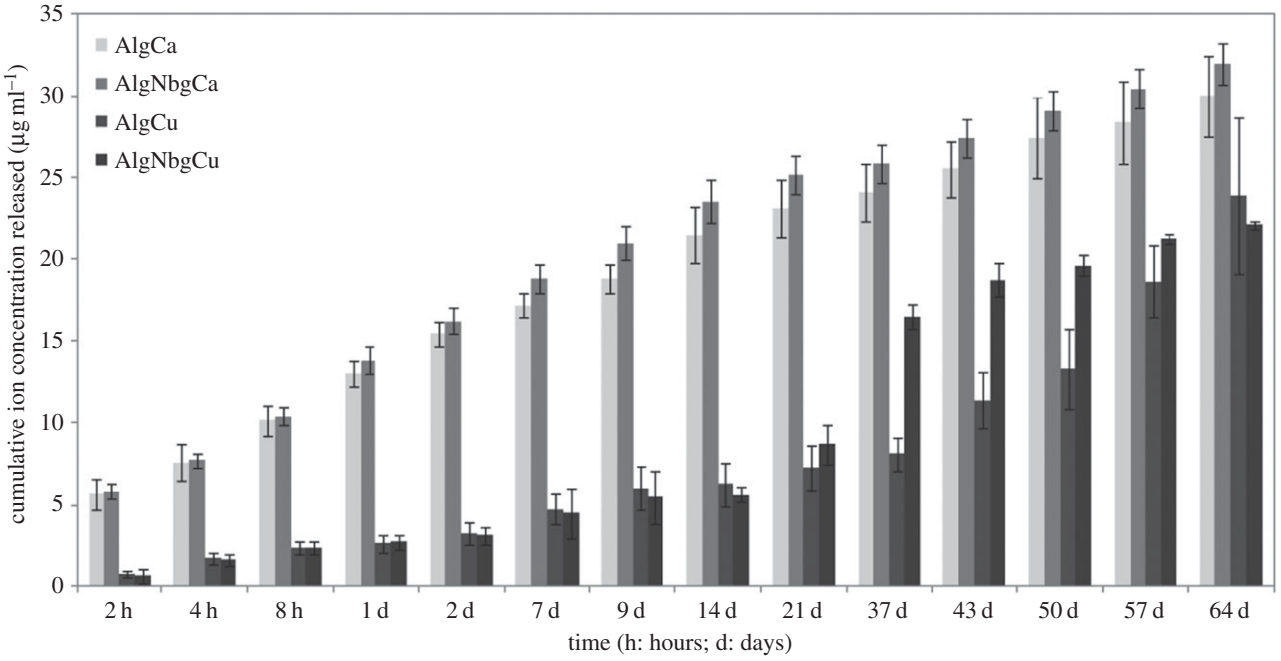

Figure 7. Cumulative release profile of Cu^{2+} and Ca^{2+} ions in phosphate buffer at pH 7.4. No significant differences for both AlgNbgCa and AlgCa 2D scaffolds were observed in the release profile. During the first three weeks of the study, the amount of Ca^{2+} ions released increased and after that and until the end of the study, a slight decrease can be noticed. Until day 21, no differences between the amount of Cu^{2+} ions released for both AlgNbgCu and AlgCu were found. From day 37 and 57, AlgNbgCu 2D scaffolds released a higher amount of Cu^{2+} ions than AlgCu 2D scaffolds. Average values $\pm$ s.d.

control; though similar results were observed at each timepoint of material incubation. Further, significant higher cell viability was observed for AlgNbgCu group compared with AlgNbgCa groups ($p < 0.001$). Similarly, it was observed that, under the influence of AlgNbgCu extracts, HUVECs produced the best results for the typical EC property of forming tubes in Matrigel both at week 1 and week 2 of being in contact. Nevertheless, HUVECs formed tubes in Matrigel in the presence of AlgNbgCa. Figure 9*b*1–*b*3 shows pictures obtained at the end of week 2, when HUVECs treated with AlgNbgCa and AlgNbgCu incubated for 1 day at 37°C in ECM were trypsinized and assayed for tube formation in Matrigel.

5. Discussion

The results of the present work suggest that the novel composite biomaterials have bioactive, biodegradable and angiogenic properties, and sufficient structural integrity to be considered for their use in the preparation of scaffolds for BTE applications.

It was demonstrated that the addition of Nbg significantly increases the tensile strength of 2D scaffolds in comparison with those without Nbg in agreement with previous studies [43,72]. This improvement of the mechanical properties could be attributed in part to the cross-linking between the Alg chains and the divalent cations from the Nbg [43], and seems to be independent of the specific multivalent ion chosen for cross-linking with the Alg. In addition, the stiffness of Alg strands can be increased by the fact that when Nbg are incorporated into Alg scaffolds, a decrease in the microporosity occurs because of their relatively high surface area [72,73]. The bioactive nature of these novel composite biomaterials was confirmed by the growth of HA crystals on the surface of 2D scaffolds when they were in contact with SBF indicating that these biomaterials might be suitable for the deposition of extracellular matrix inorganic components [25]. Moreover, degradation studies suggest that 2D scaffolds containing Ca^{2+} ions are more stable over time in comparison with those containing Cu^{2+} ions, regardless of whether Nbg are present. On the other hand, the results from the swelling study suggest that both AlgNbgCa and AlgCa 2D scaffolds have a good swelling capacity, whereas AlgNbgCu and AlgCu 2D scaffolds do not. As the Alg used in the present work was the same to prepare each type of 2D scaffolds, a possible explanation of the results obtained from both type of 2D scaffolds, containing Ca^{2+} and Cu^{2+} ions, could be attributed to differences in the interaction between the cations and the Alg residues during the cross-linking reaction. As Ca^{2+} and Cu^{2+} are divalent cations, the ion radius could play an important role in the cross-linking reaction [74]. Particularly, Alg is well known for its high affinity towards Ca^{2+} ions. Ca^{2+} ions bind consecutive guluronic residues (G-blocks) in a cooperative manner producing the cross-link of the Alg [36]. However, the cross-linking with Ca^{2+} ions is not only due to the interaction with G-blocks but also to the interaction between both mannuronic and guluronic residues (MG-blocks) [74]. By contrast, the way in which Cu^{2+} ions bind with Alg residues has not been explained so far. As Cu^{2+} ions have the same charge and a similar ion radius as zinc (Zn^{2+}) ions, it could be suggested that the cross-linking effect of Cu^{2+} ions might occur in the mannuronic residues (M-blocks) and the MG-blocks, in a similar way as was described for Zn^{2+} ions [75]. It has been reported that cations with larger ion radius can form a tighter structure in the egg-box model compared with cations of smaller ion radius as ions with larger radius are expected to fill a larger space between the blocks of Alg polymer, resulting in a tighter arrangement of cross-linked Alg matrix [74,76,77]. As Ca^{2+} ions have larger ion radius than

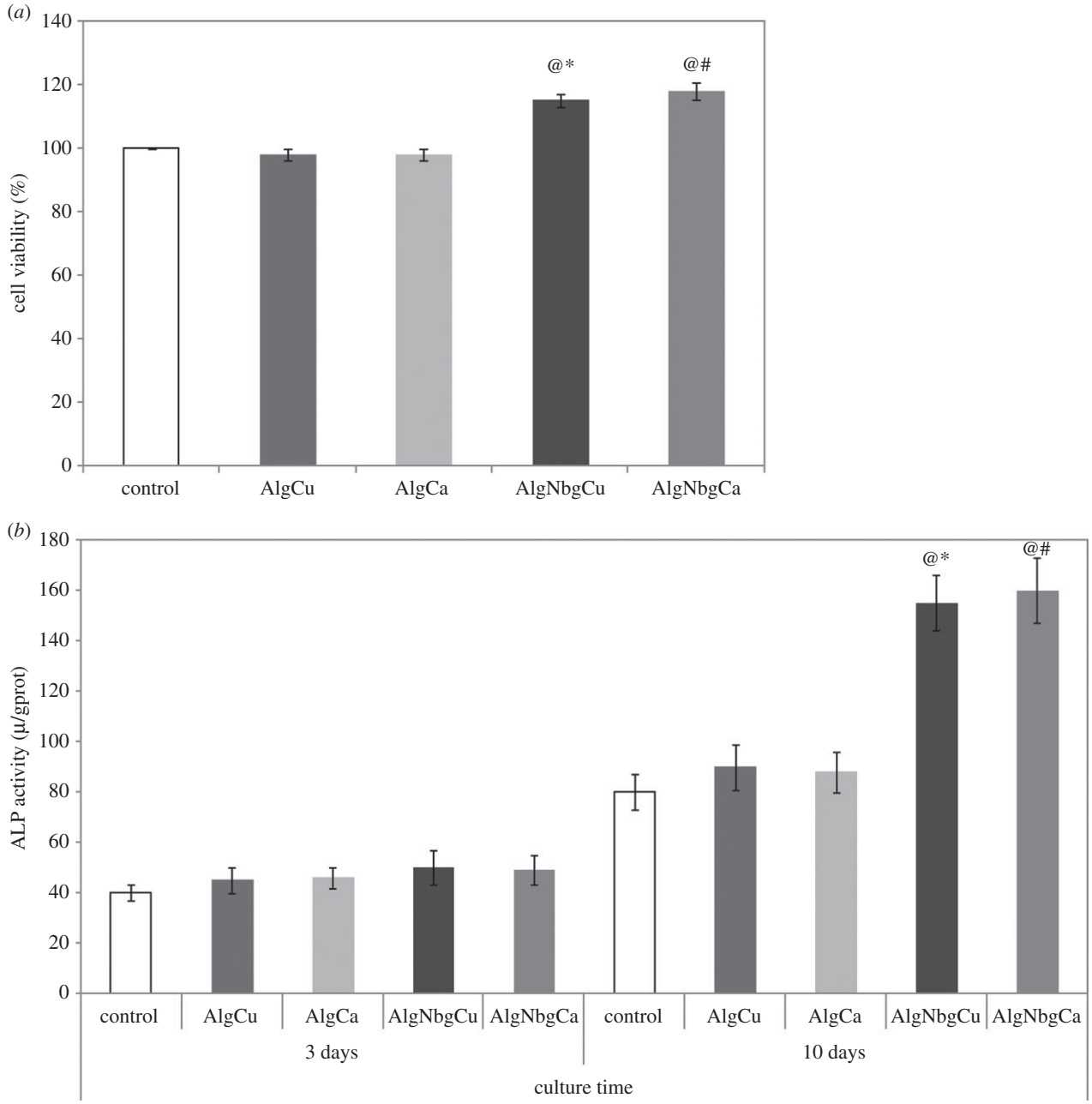

Figure 8. Effect of different extracts on the proliferation and ALP activity of rBMSCs. (*a*) Cell viability of rBMSCs cultured with different extracts for 24 h. (*b*) ALP activity of rBMSCs cultured with different extracts for 3 and 10 days. Significantly different from @, L-DMEM group; #, AlgCa group; and *, AlgCu group ($p < 0.005$). Cells cultured in L-DMEM were set as the control group. Two-dimensional scaffolds were incubated for 1 day at 37°C in L-DMEM; for results regarding other periods of incubation, refer to the text for details.

Cu^{2+} ions, this could explain the slower degradation rate obtained from 2D scaffolds containing Ca^{2+} than that of those containing Cu^{2+} ions. In addition, the results from the FTIR data of AlgNbgCu in comparison to AlgNbgCa suggest that the mass and radius of the cation play an important role in the interaction with Alg residues, due to the fact that almost all the absorption bands for AlgNbgCa were broader than those of AlgNbgCu. This might be attributed to a more stable union between Ca^{2+} ions and the COO groups from guluronic and mannuronic residues of Alg.

Regarding the swelling process, after 2D scaffolds containing Ca^{2+} are placed in the phosphate buffer medium at pH 7.4, the sodium (Na^{+}) ions present in the solution are exchanged with the Ca^{2+} ions which are binding with carboxyl groups mainly in the M-blocks [76,78]. In this way, the electrostatic repulsion among negatively charged carboxyl groups increases and causes chain relaxation and enhanced water uptake [76]. Later, the Ca^{2+} ions which are binding with carboxyl groups of the G-blocks, responsible for the egg-box model structure formation, also start to exchange with Na^{+} ions from the buffer medium and the matrix begins the degradation process [76]. The results indicate that 2D scaffolds containing Ca^{2+} ions swelled until the end of the study and the degradation process did not start until that time. By contrast, 2D scaffolds containing Cu^{2+} ions did not show any swelling properties probably because the 2D scaffolds started degrading during the first part of the swelling period, which is in agreement with the results from the degradation study.

Based on the literature previously mentioned, Ca^{2+}-cross-linked Alg gels are stable over time because of the manner in which Ca^{2+} ions interact with the G-blocks, which explains the fact that Ca^{2+}–Alg gels have been widely used for drug

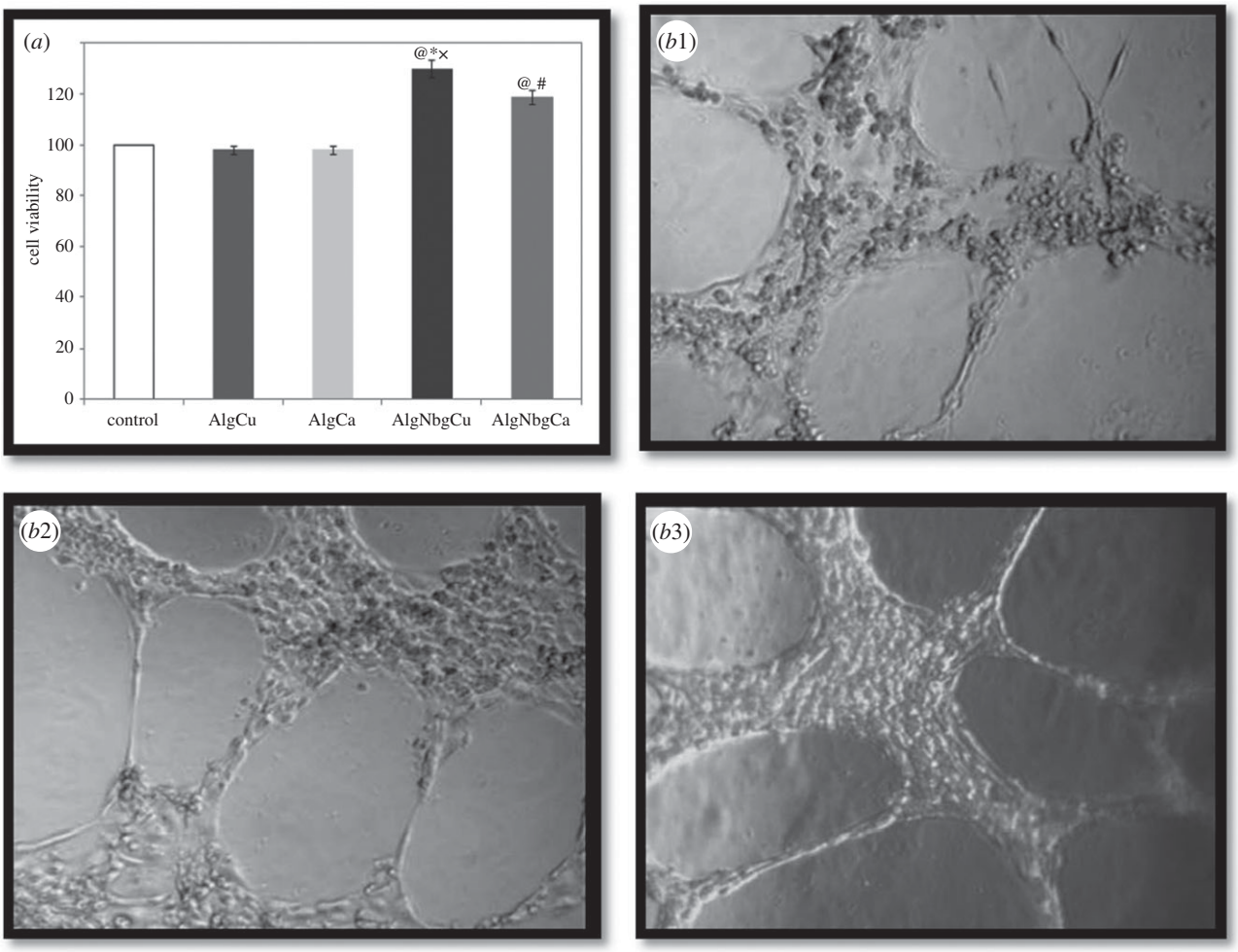

Figure 9. (*a*) Cell viability of HUVECs cultured with different 2D scaffold extracts for 24 h. Cells cultured in ECM were set as the control group. Significantly different from @, ECM group; #, AlgCa group; *, AlgCu group ($p < 0.05$); and ^{x}, AlgNbgCa group ($p < 0.001$). (*b*) HUVECs capable of forming tubes in Matrigel were pictured at the end of week 2 of being assayed: (*b*1) control, (*b*2) HUVECs in contact with AlgNbCa extract, (*b*3) HUVECs in contact with AlgNbCu extract. Similar pictures were observed also at week 1. Two-dimensional scaffolds were incubated for 1 day at 37°C in ECM; for results regarding other periods of incubation, refer to the text for details.

delivery and tissue engineering. Nevertheless, when the preparation of a multifunctional scaffold is envisaged, the possibility to use other cross-linking cations allows incorporating diverse properties based on the effects on bone formation that these cations could produce when they are released. The use of Cu^{2+} ions could have beneficial effects on bone formation and blood vessel growth [21,48]. Moreover, the use of Cu^{2+} ions as a cross-linking agent could be considered when faster degradation rates of the scaffolds are desired.

In spite of the fact that an aqueous dispersion of Nbg has high pH values, the dissolution products from 2D scaffolds containing Nbg did not produce considerable changes in the pH value of the buffer media after they are immersed, probably due to their low concentration within the composite biomaterials developed. This effect is interesting to be considered when cytocompatibility studies are being carried out, where acidic or basic pH values from the dissolution products of the biomaterials could affect the metabolism of the cells.

The results from the release study suggest that both Cu^{2+} and Ca^{2+} ions are released in a controlled manner from the 2D scaffolds without any burst release. In addition, the release of Cu^{2+} and Ca^{2+} ions was independent of the presence of Nbg, except for AlgNbgCu and AlgCu between days 37 and 57, where 2D scaffolds containing Nbg released a higher amount of Cu^{2+} ions.

As was mentioned previously, when Alg gels degrade, cross-linking cations are released due to exchange with monovalent cations from the medium [42]. Our results indicated that AlgNbgCu and AlgCu, which showed the highest degradation rates, released a lower amount of Cu^{2+} ions when compared with the amount of Ca^{2+} ions released from AlgNbgCa and AlgCa, which remained stable until the end of the degradation study. A possible explanation of this effect could be that both Cu^{2+} and Ca^{2+} ions interact with Alg chains in a different manner and with different affinity. Moreover, the fact that the amount of Ca^{2+} ions released was higher in comparison with the amount of Cu^{2+} ions released could be attributed not only to the release of Ca^{2+} ions incorporated into the 2D scaffolds, but also to the release of Ca^{2+} from the Nbg.

As described above, Cu^{2+} ions play an important role in blood vessel growth, which depends on the concentration of the ion [21,55,56]. Our results indicated that the total amount released of Cu^{2+} ions at the end of the study is within the range of values that were previously reported to stimulate the proliferation of the cell model chosen, HUVECs, without having toxic effects [21,55–57]. In the case of the release of Ca^{2+} ions, a more controlled release was observed due to the fact that Ca^{2+} ions were released steadily during the study and after 30 days the release decreased slightly in comparison with the first part

probably due to the fact that the inner part of the film was more difficult to be reached by the medium.

Regarding the *in vitro* cellular studies, the results indicate that both nanocomposite 2D scaffolds containing Cu^{2+} and Ca^{2+} ions were able to stimulate the proliferation and differentiation of rBMSCs which was confirmed by the enhancement of the activity of osteogenic markers such as ALP, when compared with AlgCu and AlgCa 2D scaffolds, respectively. Among various biological tests available to assess the differentiation of bone cells towards the osteogenic linage and to evaluate the osteoblastic activity of biomaterials, the study of the secretion and activity of ALP is an important test as this enzyme acts as one of the markers to confirm osteoblastic phenotype and mineralization [79]. ALP is an ectoenzyme produced by osteoblasts and is involved in the degradation of inorganic pyrophosphate to provide sufficient local concentration of phosphate or inorganic pyrophosphate for the mineralization process [79]. The results of this study indicated that the ALP activity from AlgNbgCu and AlgNbgCa groups was much higher after 10 days compared with the results after 3 days, suggesting that at the beginning the differentiation of bone cells had not started. In addition, as mentioned previously, it is widely known that bioactive glasses stimulate gene expression in bone cells, control the cell cycle of bone cells towards osteogenic differentiation and enhance the proliferation of osteoblasts [13,17,18]. On the other hand, both Cu^{2+} and Ca^{2+} ions are involved not only in the stimulation of proliferation of bone cells, but also in the stimulation of the differentiation of bone cells to the osteogenic linage [45,48,80]. In this sense, the synergistic effects on bone formation from Nbg and cross-linking cations would explain why these nanocomposites showed better results in comparison with those cross-linked 2D scaffolds without Nbg, and also indicating that these novel biomaterials have potential osteogenic activity of relevance for BTE scaffolds.

According to the studies to evaluate the angiogenic properties of these novel biomaterials, it is worth noticing that both Nbg and Cu^{2+} ions have important roles in blood vessel formation, which allows understanding of the results obtained. Regarding bioactive glasses, particularly those of nominally Bioglass® 45S5 composition, the effects of their ionic dissolution products on the stimulation of endothelial cell proliferation, such as HUVECs, have been widely reported [13,20]. In addition, a recent work has confirmed the effects on the promotion of blood vessel growth by bioactive glass nanoparticles with the same composition as that previously mentioned, when they are incorporated in polymer-based scaffolds for BTE [81]. These considerations are in agreement with the results of our study, where the 2D scaffolds containing Nbg showed a higher proliferation of HUVECs and a better capability of forming tubes in Matrigel in comparison with those without Nbg. Further, 2D scaffolds containing Nbg cross-linked with Cu^{2+} showed better angiogenic properties in terms of proliferation of HUVECs and forming tubes in Matrigel. Although Ca^{2+}-cross-linked composite 2D scaffolds showed angiogenic properties due only to the presence of Nbg, the enhancement of the angiogenic response due to the combination of the effects of Nbg and Cu^{2+} could be considered as a promising strategy to develop scaffolds for regenerating bone defects with highly damaged vascularization.

6. Conclusion

In this study, novel biocompatible and biodegradable nanocomposite biomaterials made of combinations of Nbg and Alg to achieve tuneable release capabilities of divalent ions—such as Cu^{2+} or Ca^{2+}—incorporated by cross-linking them with Alg were developed. The release profile of the cations showed that both Cu^{2+} and Ca^{2+} ions were released in a controlled and sustained manner with no burst release observed. In addition, the incorporation of Nbg enhanced bioactivity and improved the mechanical properties of the 2D scaffolds in comparison with those without Nbg, in agreement with previous work [43]. Finally, the *in vitro* results indicated that the bioactive ions from both nanocomposite biomaterials developed were able to stimulate rBMSC differentiation towards the osteogenic lineage and enhance HUVEC proliferation and VEGF secretion, which indicates their angiogenic properties. Novel nanocomposite biomaterials made of Nbg and Alg cross-linked with Cu^{2+} or Ca^{2+} with special focuses on controlling the release of cross-linked ions in a sustained manner were developed with potential applications in the preparation of multifunctional scaffolds for BTE.

Authors' contributions. J.P.C.: substantial contributions to conception and design, acquisition of data, analysis and interpretation of data, and drafting the article; A.H., F.P. and J.R.: acquisition of data, analysis and interpretation of data, and revising the article critically for important intellectual content; A.B.: analysis and interpretation of data, and revising the article critically for important intellectual content; S.L. and V.M.: substantial contributions to conception and design, analysis and interpretation of data, and revising the article critically for important intellectual content. All authors gave final approval of the version to be published.

Competing interests. We declare we have no competing interests.

Funding. This work was supported by grants PICT PRH 2008-138 (financed by ANPCyT, Argentina), Bilateral Cooperation Project between the University of Buenos Aires and the University of Erlangen-Nuremberg (financed by MINCyT—Argentina and BMBF—Germany), PIP 2012–2014 GI. 11220110100739 (financed by CONICET, Argentina) and partially by 'Emerging Fields Initiative' of the University of Erlangen-Nuremberg, Germany (Project TOPbiomat).

Acknowledgements. The authors acknowledge Prof. W. Stark and Dr D. Mohn for providing Nbg, and Prof. Fabián Buontempo for his help in the sterilization of the samples for the *in vitro* cellular studies.

References

1. Chen Q, Roether J, Boccaccini A. 2008 Tissue engineering scaffolds from bioactive glass and composite materials. In *Topics in tissue engineering* (eds N Ashammakhi, R Reis, F Chiellini), pp. 1–27. Oulu, Finland: Expertissues.
2. Swetha M, Sahithi K, Moorthi A, Srinivasan N, Ramasamy K, Selvamurugan N. 2010 Biocomposites containing natural polymers and hydroxyapatite for bone tissue engineering. *Int. J. Biol. Macromol.* **47**, 1–4. (doi:10.1016/j.ijbiomac.2010.03.015)

3. Allo B, Costa D, Dixon S, Mequanint K, Rizkalla A. 2012 Bioactive and biodegradable nanocomposites and hybrid biomaterials for bone regeneration. *J. Funct. Biomater.* **3**, 432–463. (doi:10.3390/jfb3020432)
4. Nezafati N, Moztarzadeh F, Hesaraki S, Moztarzadeh Z, Mozafari M. 2013 Biological response of a recently developed nanocomposite based on calcium phosphate cement and sol-gel derived bioactive glass fibers as substitution of bone tissues. *Ceram. Int.* **39**, 289–297. (doi:10.1016/j.ceramint.2012.06.024)
5. Rezwan K, Chen Q, Blaker J, Boccaccini A. 2006 Biodegradable and bioactive porous polymer/inorganic composite scaffolds for bone tissue engineering. *Biomaterials* **27**, 3413–3431. (doi:10.1016/j.biomaterials.2006.01.039)
6. Stevens M. 2008 Biomaterials for bone tissue engineering. *Mater. Today* **11**, 18–25. (doi:10.1016/S1369-7021(08)70086-5)
7. Bellucci D, Cannillo V, Sola A, Chiellini F, Gazzarri M, Migone C. 2011 Macroporous Bioglass®-derived scaffolds for bone tissue regeneration. *Ceram. Int.* **37**, 1575–1585. (doi:10.1016/j.ceramint.2011.01.023)
8. Rahaman M, Day D, Bal B, Fu Q, Jung S, Bonewald L, Tomisia A. 2011 Bioactive glass in tissue engineering. *Acta Biomater.* **7**, 2355–2373. (doi:10.1016/j.actbio.2011.03.016)
9. Chiara G, Ferroni L, Favero L, Stellini E, Stomaci D, Sivolella S, Bressan E, Zavan B. 2012 Nanostructured biomaterials for tissue engineered bone tissue reconstruction. *Int. J. Mol. Sci.* **13**, 737–757. (doi:10.3390/ijms13010737)
10. Jones J, Lin S, Yue S, Lee P, Hanna J, Smith M, Newport R. 2010 Bioactive glass scaffolds for bone regeneration and their hierarchical characterization. *Proc. Inst. Mech. Eng. Part H* **224**, 1373–1387. (doi:10.1243/09544119JEIM836)
11. Fu Q, Saiz E, Rahaman M, Tomsia A. 2011 Bioactive glass scaffolds for bone tissue engineering: state of the art and future perspectives. *Mater. Sci. Eng. C* **31**, 1245–1256. (doi:10.1016/j.msec.2011.04.022)
12. Wu C, Chang J, Xiao Y. 2011 Mesoporous bioactive glasses as drug delivery and bone tissue regeneration platforms. *Ther. Deliv.* **2**, 1189–1198. (doi:10.4155/tde.11.84)
13. Hoppe A, Güldal N, Boccaccini A. 2011 A review of the biological response to ionic dissolution products from bioactive glasses and glass-ceramics. *Biomaterials* **32**, 2757–2774. (doi:10.1016/j.biomaterials.2011.01.004)
14. Gentleman E, Stevens M, Hill R, Brauer D. 2013 Surface properties and ion release from fluoride-containing bioactive glasses promote osteoblast differentiation and mineralization *in vitro*. *Acta Biomater.* **9**, 5771–5779. (doi:10.1016/j.actbio.2012.10.043)
15. Hench L. 1998 Bioceramics. *J. Am. Ceram. Soc.* **81**, 1705–1728. (doi:10.1111/j.1151-2916.1998.tb02540.x)
16. Kokubo T, Kim H, Kawashita M. 2003 Novel bioactive materials with different mechanical properties. *Biomaterials* **24**, 2161–2175. (doi:10.1016/S0142-9612(03)00044-9)
17. Gerhardt L, Boccaccini A. 2010 Bioactive glass and glass-ceramic scaffolds for bone tissue engineering. *Materials* **3**, 3867–3910. (doi:10.3390/ma3073867)
18. Kaur G, Pandey O, Singh K, Homa D, Scott B, Pickrell G. 2013 A review of bioactive glasses: their structure, properties, fabrication and apatite formation. *J. Biomed. Mater. Res. Part A* **102**, 254–274. (doi:10.1002/jbm.a.34690)
19. Hench L. 2009 Genetic design of bioactive glass. *J. Eur. Ceram. Soc.* **29**, 1257–1265. (doi:10.1016/j.jeurceramsoc.2008.08.002)
20. Gorustovich A, Roether J, Boccaccini A. 2010 Effect of bioactive glasses on angiogenesis: a review of *in vitro* and *in vivo* evidences. *Tissue Eng. Part B* **16**, 199–207. (doi:10.1089/ten.TEB.2009.0416.)
21. Gérard C, Bordeleau L, Barralet J, Doillon C. 2010 The stimulation of angiogenesis and collagen deposition by copper. *Biomaterials* **31**, 824–831. (doi:10.1016/j.biomaterials.2009.10.009)
22. Day R. 2005 Bioactive glass stimulates the secretion of angiogenic growth factors and angiogenesis *in vitro*. *Tissue Eng.* **11**, 768–777. (doi:10.1089/ten.2005.11.768)
23. Keshaw H, Forbes A, Day R. 2005 Release of angiogenic growth factors from cells encapsulated in alginate beads with bioactive glass. *Biomaterials* **26**, 4171–4179. (doi:10.1016/j.biomaterials.2004.10.021)
24. Leach J, Kaigler D, Wang Z, Krebsbach P, Mooney D. 2006 Coating of VEGF-releasing scaffolds with bioactive glass for angiogenesis and bone regeneration. *Biomaterials* **27**, 3249–3255. (doi:10.1016/j.biomaterials.2006.01.033)
25. Boccaccini A, Erol M, Stark W, Mohn D, Hong Z, Mano J. 2010 Polymer/bioactive glass nanocomposites for biomedical applications: a review. *Compos. Sci. Technol.* **70**, 1764–1776. (doi:10.1016/j.compscitech.2010.06.002)
26. Misra S *et al.* 2010 Effect of nanoparticulate bioactive glass particles on bioactivity and cytocompatibility of poly(3-hydroxybutyrate) composites. *J. R. Soc. Interface* **7**, 453–465. (doi:10.1098/rsif.2009.0255)
27. Mackovic M, Hoppe A, Detsch R, Mohn D, Stark W, Spiecker E, Boccaccini A. 2012 Bioactive glass (type 45S5) nanoparticles: *in vitro* reactivity on nanoscale and biocompatibility. *J. Nanopart. Res.* **14**, 966. (doi:10.1007/s11051-012-0966-6)
28. Strobel L, Hild N, Mohn D, Stark W, Hoppe A, Gbureck U, Horch R, Kneser U. 2013 Novel strontium-doped bioactive glass nanoparticles enhance proliferation and osteogenic differentiation of human bone marrow stromal cells. *J. Nanopart. Res.* **15**, 1780–1788. (doi:10.1007/s11051-013-1780-5)
29. Lin H, Yeh Y. 2004 Porous alginate/hydroxyapatite composite scaffolds for bone tissue engineering: preparation, characterization, and *in vitro* studies. *J. Biomed. Mater. Res. Part B* **71**, 52–65. (doi:10.1002/jbm.b.30065)
30. Correlo V, Oliveira J, Mano J, Neves N, Reis R. 2011 Natural origin materials for bone tissue engineering—properties, processing, and performance. In *Principles of regenerative medicine* (eds A Atala, R Lanza, J Thomson, R Nerem), pp. 557–586. Amsterdam, The Netherlands: Elsevier.
31. Pérez R, Won J, Knowles J, Kim H. 2013 Naturally and synthetic smart composite biomaterials for tissue regeneration. *Adv. Drug Deliv. Rev.* **65**, 471–496. (doi:10.1016/j.addr.2012.03.009)
32. Park J. 2011 The use of hydrogels in bone-tissue engineering. *Med. Oral Patol. Oral Cir. Bucal* **16**, 115–118. (doi:10.4317/medoral.16.e115)
33. Augst A, Kong H, Mooney D. 2006 Alginate hydrogels as biomaterials. *Macromol. Biosci.* **6**, 623–633. (doi:10.1002/mabi.200600069)
34. Baroli B. 2007 Hydrogels for tissue engineering and delivery of tissue inducing substances. *J. Pharm. Sci.* **96**, 2197–2223. (doi:10.1002/jps.20873)
35. Place E, Rojo L, Gentleman E, Sardinha J, Stevens M. 2011 Strontium- and zinc-alginate hydrogels for bone tissue engineering. *Tissue Eng. Part A* **17**, 2713–2722. (doi:10.1089/ten.TEA.2011.0059)
36. Andersen T, Strand B, Formo K, Alsberg E, Christensen B. 2012 Alginates as biomaterials in tissue engineering. In *Carbohydrate chemistry* (eds A Rauter, T Lindhorst), pp. 227–258. London, UK: RSC Publishing.
37. Florczyk S, Leung M, Jana S, Li Z, Bhattarai N, Huang J, Hopper R, Zhang M. 2012 Enhanced bone tissue formation by alginate gel-assisted cell seeding in porous ceramic scaffolds and sustained release of growth factor. *J. Biomed. Mater. Res. Part A* **100**, 3408–3415. (doi:10.1002/jbm.a.34288)
38. Valente J, Valente T, Alves P, Ferreira P, Silva A, Correia I. 2012 Alginate based scaffolds for bone tissue engineering. *Mater. Sci. Eng. C* **32**, 2596–2603. (doi:10.1016/j.msec.2012.08.001)
39. Morais D, Rodrigues M, Silva T, Lopes M, Santos M, Santos J, Botelho C. 2013 Development and characterization of novel alginate-based hydrogels as vehicles for bone substitutes. *Carbohydr. Polym.* **95**, 134–142. (doi:10.1016/j.carbpol.2013.02.067)
40. Sachan N, Pushkar S, Jha A, Bhattcharya A. 2009 Sodium alginate: the wonder polymer for controlled drug delivery. *J. Pharm. Res.* **2**, 1191–1199.
41. Chen C-HD, Chen C-C, Shie M-Y, Huang C-H, Ding S-J. 2011 Controlled release of gentamicin from calcium phosphate/alginate bone cement. *Mater. Sci. Eng. C* **31**, 334–341. (doi:10.1016/j.msec.2010.10.002)
42. Lee K, Mooney D. 2012 Alginate: properties and biomedical applications. *Prog. Polym. Sci.* **37**, 106–126. (doi:10.1016/j.progpolymsci.2011.06.003)
43. Mouriño V, Newby P, Pishbin F, Cattalini J, Lucangioli S, Boccaccini A. 2011 Physicochemical, biological and drug-release properties of gallium crosslinked alginate/nanoparticulate bioactive glass composite 2D scaffolds. *Soft Matter* **7**, 6705–6712. (doi:10.1039/C1SM05331 K)
44. Lakhkar N, Lee I, Kim H, Salih V, Wall I, Knowles J. 2013 Bone formation controlled by biologically relevant inorganic ions: role and controlled delivery

from phosphate-based glasses. *Adv. Drug Deliv. Rev.* **65**, 405–420. (doi:10.1016/j.addr.2012.05.015)

45. Mouriño V, Cattalini JP, Boccaccini AR. 2012 Metallic ions as therapeutic agents in tissue engineering scaffolds: an overview of their biological applications and strategies for new developments. *J. R. Soc. Interface* **9**, 401–419. (doi:10.1098/rsif.2011.0611)
46. Erol M, Özyuguran A, Özarpat Ö, Kücükbayrak S. 2012 3D Composite scaffolds using strontium containing bioactive glasses. *J. Eur. Ceram. Soc.* **32**, 2747–2755. (doi:10.1016/j.jeurceramsoc.2012.01.015)
47. Erol M, Mouriño V, Newby P, Chatzistavrou X, Roether J, Hupa L, Boccaccini A. 2012 Copper-releasing, boron-containing bioactive glass-based scaffolds coated with alginate for bone tissue engineering. *Acta Biomater.* **8**, 792–801. (doi:10.1016/j.actbio.2011.10.013)
48. Wu C, Zhou Y, Fan W, Han P, Chang J, Yuen J, Zhang M, Xiao Y. 2012 Hypoxia-mimicking mesoporous bioactive glass scaffolds with controllable cobalt ion release for bone tissue engineering. *Biomaterials* **33**, 2076–2085. (doi:10.1016/j.biomaterials.2011.11.042)
49. Hoppe A, Mouriño V, Boccaccini A. 2013 Therapeutic inorganic ions in bioactive glasses to enhance bone formation and beyond. *Biomater. Sci.* **1**, 254–256. (doi:10.1039/C2BM00116 K)
50. Maeno S, Niki Y, Matsumoto H, Morioka H, Yatabe T, Funayama A, Toyama Y, Taguchi T, Tanaka J. 2005 The effect of calcium ion concentration on osteoblast viability, proliferation and differentiation in monolayer and 3D culture. *Biomaterials* **26**, 4847–4855. (doi:10.1016/j.biomaterials.2005.01.006)
51. Marie P. 2010 The calcium-sensing receptor in bone cells: a potential therapeutic target in osteoporosis. *Bone* **46**, 571–576. (doi:10.1016/j.bone.2009.07.082)
52. Finney L, Vogt S, Fukai T, Glesne D. 2009 Copper and angiogenesis: unravelling a relationship key to cancer progression. *Clin. Exp. Pharmacol. Physiol.* **36**, 88–94. (doi:10.1111/j.1440-1681.2008.04969.x)
53. Barrelet J, Gbureck U, Habibovic P, Vorndran E, Gérard C, Doillon C. 2009 Angiogenesis in calcium phosphate scaffolds by inorganic copper ion release. *Tissue Eng. Part A* **15**, 1601–1609. (doi:10.1089/ten.tea.2007.0370)
54. Wu C, Zhou Y, Xu M, Han P, Chen L, Chang J, Xiao Y. 2013 Copper-containing mesoporous bioactive glass scaffolds with multifunctional properties of angiogenesis capacity, osteostimulation and antibacterial activity. *Biomaterials* **34**, 422–433. (doi:10.1016/j.biomaterials.2012.09.066)
55. Hu G. 1998 Copper stimulates proliferation of human endothelial cells under culture. *J. Cell. Biochem.* **69**, 326–335. (doi:10.1002/(SICI)1097-4644(19980601)69:3<326::AID-JCB10>3.0.CO;2-A)
56. Bar-Or D, Thomas D, Yukl R, Rael L, Shimonkevitz R, Curtis C, Winkler J. 2003 Copper stimulates the synthesis and release of interleukin-8 in human endothelial cells: a possible early role in systemic inflammatory responses. *Shock* **20**, 154–158. (doi:10.1097/01.shk.0000068318.49350.3a)
57. Li S, Xie H, Li S, Kang Y. 2012 Copper stimulates growth of human umbilical vein endothelial cells in a vascular endothelial growth factor-independent pathway. *Exp. Biol. Med.* (*Maywood*) **237**, 77–82. (doi:10.1258/ebm.2011.011267)
58. Kong N, Lin K, Li H, Chang J. 2014 Synergy effects of copper and silicon ions on stimulation of vascularisation by copper-doped calcium silicate. *J. Mater. Chem. B* **2**, 1100–1110. (doi:10.1039/C3TB21529F)
59. Rodríguez J, Ríos S, González M. 2002 Modulation of the proliferation and differentiation of human mesenchymal stem cells by copper. *J. Cell. Biochem.* **85**, 92–100. (doi:10.1002/jcb.10111)
60. Esteban-Tejeda L, Malpartida F, Esteban-Cubillo A, Pecharromán C, Moya JS. 2009 Antibacterial and antifungal activity of a soda-lime glass containing copper nanoparticles. *Nanotechnology* **20**, 505701. (doi:10.1088/0957-4484/20/50/505701)
61. Mouriño V, Boccaccini AR. 2010 Bone tissue engineering therapeutics: controlled drug delivery in three-dimensional scaffolds. *J. R. Soc. Interface* **7**, 209–227. (doi:10.1098/rsif.2009.0379)
62. Srinivasan S, Jayasree R, Chennazhi K, Nair S, Jayakumar R. 2012 Biocompatible alginate/nano bioactive glass ceramic composite scaffolds for periodontal tissue regeneration. *Carbohydr. Polym.* **87**, 274–283. (doi:10.1016/j.carbpol.2011.07.058)
63. Brunner T, Grass R, Stark W. 2006 Glass and bioglass nanopowders by flame synthesis. *Chem. Commun.* 1384–1386. (doi:10.1039/B517501A)
64. Baraj B, Martínez M, Sastre A, Aguilar M. 1995 Simultaneous determination of Cr(III), Fe(III), Cu(II) and Pb(II) as UV-absorbing EDTA complexes by capillary zone electrophoresis. *J. Chromatogr. A* **695**, 103–111. (doi:10.1016/0021-9673(94)01078-S)
65. Cattalini J, García J, Mouriño V, Lucangioli S. 2014 Development and validation of a capillary zone electrophoresis method for the determination of calcium in composite biomaterials. *Curr. Anal. Chem.* **10**, 465–472. (doi:10.2174/1573411013099990038)
66. Frank O, Heim M, Jacob M, Barbero A, Schäfer D, Bendik I, Dick W, Heberer M, Martin I. 2002 Real-time quantitative RT-PCR analysis of human bone marrow stromal cells during osteogenic differentiation *in vitro*. *J. Cell. Biochem.* **85**, 737–746. (doi:10.1002/jcb.10174)
67. Smejkal G, Kaul C. 2001 Stability of nitro blue tetrazolium-based alkaline phosphate substrates. *J. Histochem. Cytochem.* **49**, 1189–1190. (doi:10.1177/002215540104900914)
68. Morton R, Evans T. 1992 Modification of the bicinchoninic acid protein assay to eliminate lipid interface in determining lipoprotein protein content. *Anal. Biochem.* **204**, 332–334. (doi:10.1016/0003-2697(92)90248-6)
69. Cerruti M, Greenspan D, Powers K. 2005 Effect of pH and ionic strength on the reactivity of Bioglass® 45S5. *Biomaterials* **26**, 1665–1674. (doi:10.1016/j.biomaterials.2004.07.009)
70. Du H, Williams C, Ebner A, Ritter J. 2010 *In situ* FTIR spectroscopic analysis of carbonate transformations during adsorption and desorption of CO_2 in K-promoted HTlc. *Chem. Mater.* **22**, 3519–3526. (doi:10.1021/cm100703e)
71. Tan H, Kacey G. 2010 Injectable biodegradable hydrogels for tissue engineering applications. *Materials* **3**, 1746–1767. (doi:10.3390/ma3031746)
72. Luo Y, Wu C, Lode A, Gelinsky M. 2013 Hierarchical mesoporous bioactive glass/alginate composite scaffolds fabricated by three-dimensional plotting for bone tissue engineering. *Biofabrication* **5**, 015005. (doi:10.1088/1758-5082/5/1/015005)
73. Misra S, Mohn D, Brunner T, Stark W, Philip S, Roy I, Salih V, Knowles J, Boccaccini A. 2008 Comparison of nanoscale and microscale bioactive glass on the properties of P(3HB)/Bioglass® composites. *Biomaterials* **29**, 1750–1761. (doi:10.1016/j.biomaterials.2007.12.040)
74. Yang C, Wang M, Haider H, Yang J, Sun J, Chen Y, Zhou J, Suo Z. 2013 Strengthening alginate/polyacrylamide hydrogels using various multivalent cations. *ACS Appl. Mater. Interfaces* **5**, 10 418–10 422. (doi:10.1021/am403966x)
75. McDowell R. 1977 *Properties of alginates*, 4th edn. London, UK: Alginate Industries Limited.
76. Bajpai S, Sharma S. 2004 Investigation of swelling/degradation behaviour of alginate beads crosslinked with Ca^{2+} and Ba^{2+} ions. *React. Funct. Polym.* **59**, 129–140. (doi:10.1016/j.reactfunctpolym.2004.01.002)
77. Na Y, Tanaka Y, Kawauchi Y, Furukawa H, Sumiyoshi T, Gong J, Osada Y. 2006 Necking phenomenon of double-network gels. *Macromolecules* **39**, 4641–4645. (doi:10.1021/ma060568d)
78. Mørch Y, Donati I, Strand B, Skjak-Bræk G. 2006 Effect of Ca^{2+}, Ba^{2+}, and Sr^{2+} on alginate microbeads. *Biomacromolecules* **7**, 1471–1480. (doi:10.1021/bm060010d)
79. Wutticharoenmongkol P, Pavasant P, Supapho P. 2007 Osteoblastic phenotype expression of mc3t3-e1 cultured on electrospun polycaprolactone fiber mats filled with hydroxyapatite nanoparticles. *Biomacromolecules* **8**, 2602–2610. (doi:10.1021/bm700451p)
80. Ewald A, Kappel C, Vorndran E, Moseke C, Gelinsky M, Gbureck U. 2012 The effect of Cu(II)-loaded brushite scaffolds on growth and activity of osteoblastic cells. *J. Biomed. Mater. Res. A* **100**, 2392–2400. (doi:10.1002/jbm.a.34184)
81. Vargas G *et al.* 2013 Effect of nano-sized bioactive glass particles on the angiogenic properties of collagen based composites. *J. Mater. Sci. Mater. Med.* **24**, 1261–1269. (doi:10.1007/s10856-013-4892-7)